



# Variational Assimilation of Land Surface Temperature within the ORCHIDEE Land Surface Model Version 1.2.6

H. S. Benavides Pinjosovsky<sup>1,2,3</sup>, S. Thiria<sup>1</sup>, C. Ottlé<sup>2</sup>, J. Brajard<sup>1</sup>, F. Bradran<sup>1</sup> and P. Maugis<sup>2</sup>

<sup>1</sup>Laboratoire d'Océanographie et du Climat: Expérimentations et Approches Numériques, IPSL Paris, France}

<sup>2</sup>Laboratoire des Sciences du Climat et de l'Environnement, IPSL, CNRS-CEA-UVSQ, Gif-sur-Yvette, France}

<sup>3</sup>CLIMMOD Engineering}, Orsay, France

Correspondence to: H. S. Benavides Pinjosovsky ([spinjosovsky@gmail.com](mailto:spinjosovsky@gmail.com)) and S. Thiria ([sylvie.thiria@locean-ipsl.upmc.fr](mailto:sylvie.thiria@locean-ipsl.upmc.fr))

**Abstract.** The SECHIBA module of the ORCHIDEE land surface model describes the exchanges of water and energy between the surface and the atmosphere. In the present paper, the adjoint semi-generator software denoted YAO was used as a framework to implement a 4D-VAR assimilation method. The objective was to deliver the adjoint model of SECHIBA (SECHIBA-YAO) obtained with YAO to provide an opportunity for scientists and end users to perform their own assimilation. SECHIBA-YAO allows the control of the eleven most influent internal parameters of SECHIBA or of the initial conditions of the soil water content by observing the land surface temperature measured in situ or as it could be observed by remote sensing as brightness temperature. The paper presents the fundamental principles of the 4D-Var assimilation, the semi-generator software YAO and some experiments showing the accuracy of the adjoint code distributed. In addition, a distributed version is available when only the land surface temperature is observed.

**Keywords:** Sensitivity Analysis, Data Assimilation, Adjoint model, Land Surface Temperature

## 1. Introduction

Land surface models (LSM) simulate the interactions between the atmosphere and the land surface, which directly influence the exchange of water, energy and carbon with the atmosphere. They are important tools for understanding the main interaction and feedback processes simulating the present climate and making predictions of future climate evolution (Harrison et al., 2009). Such predictions are subject to considerable uncertainties, related to the difficulty to model the highly complex physics with a limited set of equations that does not account for all the interacting processes (Pipunic et al., 2008, Ghent et al. 2011). Understanding these uncertainties is important in order to obtain more realistic simulations.

The main challenge of a dynamical model, regardless its nature, is to have the appropriate source of information to produce an accurate response. Observations sample the system of interest in space and time. These measurements provide essential information on the model dynamics and contribute to the understanding of the system evolution (Lahoz et al. 2010). Data assimilation adds observations to the model, constraining it to represent the trajectory of the modeled phenomena more accurately. The objective is to merge the measurements with the dynamical model in order to obtain a more accurate estimate of the current and future states of the system, given the model and observations uncertainties. Two basic methodologies can be used for that purpose. The sequential approach (Evensen 2003), based on the statistical estimation theory of the Kalman filter, and the variational approach, the so-called 4DVAR (Le Dimet et al., 1986), built from the optimal control theory (Robert et al, 2007). It is well known that both approaches provide the same solution at



1 the end of the assimilation period, for perfect and linear models. But both approaches become very different when the  
2 processes under study are highly nonlinear. The main advantage of 4DVAR comes from its integration in time achieved  
3 during the assimilation of the observations, giving rise to a global trajectory of the model optimized over the assimilation  
4 time window.

5 Variational data assimilation has been widely used in land surface applications. The assimilation of land surface  
6 temperature (LST) is suitable for an extensive range of environmental problems. As mentioned in Ridler et al. (2012),  
7 LST is an excellent candidate for model optimization since it is solution of the coupled energy and water budgets, and  
8 permits to constrain parameters related to evapotranspiration and indirectly to soil water content. In Castelli et al. (1999),  
9 a variational data assimilation approach is used to include surface energy balance in the estimation procedure as a  
10 physical constraint (based on adjoint techniques). The authors worked with satellite data, and directly assimilated soil  
11 skin temperatures. They conclude that constraining the model with such observations improves model flux estimates,  
12 with respect to available measurements. In Huang et al. (2003) the authors developed a one-dimensional land data  
13 assimilation scheme based on an ensemble Kalman filter, used to improve the estimation of land surface temperature  
14 profile. They demonstrate that the assimilation of LST into land surface models is a practical and effective way to  
15 improve the estimation of land surface state variables and fluxes. Reichle et al. (2010) performs the assimilation of  
16 satellite-derived skin temperature observations using an ensemble-based, offline land data assimilation system. Results  
17 suggest that the retrieved fluxes provide modest but statistically significant improvements. However, these authors noted  
18 strong biases between LST estimates from *in situ* observations, land modeling, and satellite retrievals that vary with  
19 season and time of the day. They highlighted the importance of taking these biases into account. Otherwise large errors in  
20 surface flux estimates can result. Ghent et al. (2011) investigated the impacts of data assimilation on terrestrial feedbacks  
21 of the climate system. Assimilation of LST helped to constrain simulations of soil moisture and surface heat fluxes.  
22 Ridler et al. (2012), tested the effectiveness of using satellite estimates of radiometric surface temperatures and surface  
23 soil moisture to calibrate a Soil–Vegetation–Atmosphere Transfer (SVAT) model, based on error minimization of  
24 temperature and soil moisture model outputs. Flux simulations were improved when the model is calibrated against *in*  
25 *situ* surface temperature and surface soil moisture versus satellite estimates of the same fluxes. In Bateni et al. (2013), the  
26 full heat diffusion equation is employed in the variational data assimilation scheme as an adjoint (constraint). Deviations  
27 terms of the evaporation fraction and a scale coefficient are added as penalization terms in the cost function. Weak  
28 constraint is applied to data assimilation with model uncertainty, accounting in this way for model errors. The cost  
29 function associated with this experiment contains a term that penalizes the deviation from prior values. When  
30 assimilating LST into the model, the authors proved that the heat diffusion coefficients are strongly sensitive to specific  
31 deep land surface temperature. As a conclusion, it can be seen that the assimilation of LST can improve the model  
32 simulated flows.

33 In the present study, we focused on the SECHIBA module (Ducoudré et al. 1993), part of the ORCHIDEE Land Surface  
34 Model, dedicated to the resolution of the surface energy and water budgets. Our objective was to test the ability of  
35 4DVAR to estimate a set of its inner parameters as well as initial conditions of surface soil water content by observing  
36 the brightness temperature or the soil temperature. A dedicated software (denoted SECHIBA-YAO) was developed by  
37 using the adjoint semi-generator software denoted YAO developed at LOCEAN-IPSL (Nardi et al. 2009). YAO serves as  
38 a framework to design and implement dynamic models, helping to generate the adjoint of the model which permits to  
39 compute the model gradients. SECHIBA-YAO provides an opportunity to control the most influent internal parameters  
40 of SECHIBA by assimilating land surface temperature observations. At a given location and for specific soil and climate



1 conditions, twin experiments or assimilation with remote sensing data can be executed. The twin experiments conducted  
2 on actual sites were used to demonstrate the accuracy and usefulness of the code and the potential of 4D-VAR when  
3 dealing with LST assimilation. The assimilation tools are available introduced in Section 5.

4 This paper is structured as follows. In Section 2, model and data used to illustrate the capabilities of the SECHIBA-YAO  
5 are detailed. In Section 3, fundamentals of variational data assimilation are presented. In addition, principles of YAO and  
6 of its associated modular graph formalism are exposed. The principle of the computation of the adjoint with YAO is  
7 provided. The implementation of SECHIBA-YAO and the details of the experiments that prove the efficiency of the 4D-  
8 Var assimilation, are also subject of Section 3. Sensitivity experiments and simple twin experiments at a single location  
9 are presented in Section 4. These experiments illustrate the convenience of YAO to optimize control parameters. Finally,  
10 the specificities of the distributed software are given in Section 5.

## 11 2. Models and Data

12 ORCHIDEE is a Land Surface Model developed at the “Institut Pierre Simon Laplace (IPSL)” in France. ORCHIDEE is  
13 a mechanistic dynamic global vegetation model (Krinner et al., 2005) representing the continental biosphere and its  
14 different biophysical processes. It is part of the IPSL earth system model (LMDZ, Hourdin et al., 2006), and is composed  
15 of 3 modules: SECHIBA, STOMATE and LPJ. The version used to this work correspond to the version 1.2.6, released  
16 the 22th April 2010. SECHIBA computes the water and energy budgets at the biosphere-atmosphere interface, as well as  
17 the Gross Primary Production (GPP); STOMATE (Friedlingstein et al., 1999) is a biogeochemical model which  
18 represents the processes related to the carbon cycle, such as carbon dynamics, the allocation of photosynthesis respiration  
19 and growth maintenance, heterotrophic respiration and phenology and finally, LPJ (Sitch et al., 2003) models the global  
20 dynamics of the vegetation, interspecific competition for sunlight as well as fire occurrence. ORCHIDEE has different  
21 time scales: 30-minutes for energy and matter, 1-day for carbon processes and 1-year for species competition processes.  
22 The full description of ORCHIDEE can be found in Ducoudré et al., 1993, Krinner et al., 2005, d’Orgeval et al., 2006,  
23 Kuppel et al., 2012. In the present study, ORCHIDEE 1.9 version is used in a grid-point mode (one given location),  
24 forced by the corresponding local half-hourly gap-filled meteorological measurements obtained at the flux towers. In this  
25 study, only the SECHIBA module is considered.

26 In SECHIBA, the land surface is represented as a whole system composed of various fractions of vegetation types called  
27 PFT (Plant Functional Type). A single energy budget is performed for each grid point, but water budget is calculated for  
28 each PFT fraction. The resulting energy and water fluxes between atmosphere, ground and the retrieved temperature  
29 represent the canopy ensemble and the soil surface. The main fluxes modeled are the net radiation ( $R_n$ ), soil heat flux ( $Q$ ),  
30 sensible ( $H$ ) and latent heat ( $LE$ ) fluxes between the atmosphere and the biosphere, land surface temperature ( $LST$ ) and  
31 the soil water reservoir contents. Energy balance is solved once, with a subdivision only for  $LE$  in bare soil evaporation,  
32 interception and transpiration for each type of vegetation. Water balance is computed for each fraction of vegetation  
33 (Plant Functional Type or PFT) present in the grid. The SECHIBA version used in this work models the hydrological  
34 budget based on a two-layer soil profile (Choisnel, 1977). The two soil layers represent respectively the surface and the  
35 total rooting zone. The soil is considered homogeneous with no sub-grid variability and of a total depth of  $h_{tot} = 2m$ . The  
36 soil bottom layer acts like a bucket that is filled with water from the top layer. The soil is filled from top to bottom with  
37 precipitation; when evapotranspiration is higher than precipitation, water is removed from the upper reservoir. Runoff  
38 arises when the soil is saturated. SECHIBA inputs are:  $R_{lw}$  the incoming infrared radiation;  $R_{sw}$  the incoming solar  
39 radiation;  $P$  the total precipitation (rain and snow);  $T_a$  the air temperature;  $Q_a$  the air humidity;  $P_s$  the atmospheric  
40 pressure at the surface and  $U$  the wind speed.



1 In the full version of SECHIBA-YAO, observations of LST or brightness temperature can be used to constrain model  
 2 inner parameter or initial conditions of the model variables. However, the simulated LST is hemispheric and does not  
 3 account for solar configuration and viewing angle effects. In order to compute a thermal infrared brightness temperature  
 4 from LST, and neglecting the directional effects, the total energy emitted by the surface (Rad) can be computed using the  
 5 following expression :

$$6 \quad Rad = k_{emis} \varepsilon LST^4 + (1 - \varepsilon k_{emis}) LW_{down} \quad (\text{Eq 1})$$

7  
 8 In this equation,  $\varepsilon$  is the surface emissivity,  $k_{emis}$  is the multiplicative factor for emissivity and  $LW_{down}$  is the longwave  
 9 incident radiation that is an input forcing of SECHIBA. Svendsen et al. (1990) proposed a transfer function to link the  
 10 surface emitted radiance towards an observed brightness temperature  $TB$  measured in the [8,14]  $\mu\text{m}$  spectral band The  
 11 empirical formulation is given by the expression

$$12 \quad TB = \left( \frac{Rad - 7.84}{6.7975 \cdot 10^{11}} \right)^{0.2} \quad (\text{Eq 2})$$

13 In the following the capabilities of the 4D-VAR is demonstrated in a series of assimilation experiment using the data  
 14 provided by the FLUXNET network. SECHIBA-YAO can be run using other data as long as the inputs needed to operate  
 15 SECHIBA are completed. FLUXNET (Baldocchi et al., 2001) is a network coordinating regional and global analysis of  
 16 observations from micrometeorological tower sites. The flux tower sites use eddy covariance methods (Aubinet et al.  
 17 2012) to measure the exchange of carbon dioxide ( $\text{CO}_2$ ), water vapor, and energy between terrestrial ecosystems and the  
 18 atmosphere.

19 Measurement towers sprang up around the world, grouped in regional networks. The data from all networks is accessible  
 20 to the scientific community via the Fluxnet website (<http://www.fluxdata.org>). In this work, we selected 2 sites: Harvard  
 21 Forest and Skukuza Kruger National Park; both present contrasted climate and land surface properties suitable to test the  
 22 tools developed and assess model parameters sensitivities. Only climate measurements with the same sampling frequency  
 23 (30 minutes) from both sites are used to force SECHIBA. Vegetation characteristics are prescribed and only  
 24 homogeneous grids are considered. Two cases were studied with agricultural C3 (PFT 12) and bare soil (PFT 1).

#### 25 *Skukuza Kruger National Park*

26 Located in South Africa at  $25^\circ 1' 11''$  S and  $31^\circ 29' 48''$  E, , this Fluxnet site was established in 2000. The tower overlaps  
 27 two distinct savanna types and collects information about land-atmosphere interactions. The climate is Subtropical-  
 28 Mediterranean. The total mean annual precipitation is 650 mm, with an altitude of 150 m and the mean annual  
 29 temperature is  $22.15^\circ\text{C}$ .

#### 30 *Harvard Forest*

31 Located in the United States of America, on land owned by Harvard University, the station is located at  $42^\circ 53' 78''$  N and  
 32  $72^\circ 17' 15''$  W. It was established in 1991. The site has a Temperate-Continental climate with hot or warm summers and  
 33 cold winters. The annual mean precipitation is 1071 mm, the mean annual temperature is  $6.62^\circ\text{C}$  and the altitude is 340  
 34 m.

35



1 **3. The Methodology**

2 **3.1 Variational assimilation**

3 Variational assimilation (4D-VAR) (Le Dimet et al. 1986) considers a physical phenomenon described in space and its  
 4 time evolution. It thus requires the knowledge of a direct dynamical model  $M$ , which describes the time evolution of the  
 5 physical phenomenon.  $M$  allows connecting the geophysical variables studied with observations. By varying some  
 6 geophysical variables (control variables); assimilation seeks to infer the physical variables that led to the observation  
 7 values. These physical variables can be, for example, initial conditions or parameters of  $M$ .

8 The basic idea is to determine the minimum of a cost function  $J$  that measures the misfits between the observations and  
 9 the model estimations. Due to the complexity of this function, the solution is classically obtained by using gradient  
 10 methods, which implies the use of the adjoint model of  $M$ . This model is derived from the equations of the direct model  
 11  $M$ . The adjoint model estimates changes in the control variables in response to a disturbance of the output values  
 12 calculated by  $M$ . It is therefore necessary to proceed in the backward direction to the direct model calculations, which  
 13 means to use the transpose of the Jacobean matrix with respect to the control parameters. When observations are  
 14 available, the adjoint allows minimizing the cost function  $J$ .

15 Formalism and notations for variational data assimilation are taken from Ide et al., (1997).  $M$  represents the direct model,  
 16  $\mathbf{x}(t_0)$  is the initial state of the model and  $\mathbf{k}$  represents the vector of the inner model parameters to be controlled, so  $\mathbf{x}(t_i) =$   
 17  $M_i(\mathbf{k}, \mathbf{x}(t_0))$ , where  $M_i(\mathbf{k}, \mathbf{x}(t_0))$  is represented by  $M \circ M \circ \dots \circ M(\mathbf{k}, \mathbf{x}(t_0))$ . The tangent linear model is noted  
 18  $\mathbf{M}(t_i, t_{i+1})$ , which is the Jacobean matrix of  $\mathbf{M}$ , in  $\mathbf{x}(t_i)$ . The adjoint model  $\mathbf{M}_i^T$  is the linear tangent transpose, defined as:

19 
$$\mathbf{M}_i^T = \prod_{j=0}^{i-1} \mathbf{M}(t_j, t_{j+1})^T \quad \text{Eq. (3)}$$

20  $\mathbf{M}$  is used to estimate variables, which are most often observed from an observation operator  $\mathbf{H}$ , permitting to compare  
 21 the observed values  $\mathbf{y}^0$  with respect to the  $\mathbf{y}$  calculated by the composition  $\mathbf{H} \circ \mathbf{M}$ , when they are available. The cost  
 22 function  $J$  will be defined in terms of observations, so  $\mathbf{H}_i$  allows us to estimate the variables  $\mathbf{y}_i$  from the state vector  $\mathbf{x}(t_i)$ .

23 We suppose that  $\mathbf{y}_i = \mathbf{H}_i(\mathbf{M}_i(\mathbf{x}_i, \mathbf{k})) + \varepsilon$  where  $\varepsilon_i$  is a random variable with zero mean. This term represents the sum  
 24 of the model, observation and scaling error. Finally, the most general form of the cost function is defined as follows:

25 
$$J(\mathbf{k}) = \frac{1}{2} (\mathbf{k} - \mathbf{k}^b)^T \mathbf{B}^{-1} (\mathbf{k} - \mathbf{k}^b) + \frac{1}{2} \sum_{i=0}^t (\mathbf{y}_i - \mathbf{y}_i^0)^T \mathbf{R}_i^{-1} (\mathbf{y}_i - \mathbf{y}_i^0) \quad \text{Eq. (4)}$$

26 The background vector is defined as  $\mathbf{k}^b$ , which is an *a priori* vector of the inner model parameters. The first part of the  
 27 cost function represents the discrepancy to  $\mathbf{k}^b$  and acts as a regularization term. The second part represents the distance  
 28 between the observations and the model estimates.  $\mathbf{B}$  is the covariance error matrix of  $\mathbf{k}^b$  and  $\mathbf{R}_i$  is the covariance error  
 29 matrix of  $\mathbf{y}^0$  at time  $t_i$ . The objective of this work is to show the capacity of 4DVAR to help determining the value of the  
 30 principal inner parameters  $\mathbf{k}$  of SECHIBA and the initial conditions for Surface Water Content. The present distributed  
 31 software allows the reader to do its own experiments using synthetic or actual data. When the observations are synthetic  
 32 (produced by the model itself) no transfer function from the estimation to the observation are needed, and  $\mathbf{H}$  is taken as  
 33 the identity matrix. If actual data are used, a specific  $\mathbf{H}$  is used that transforms the soil temperature into brightness  
 34 temperature (see section Model and Data).



1 The minimization of the cost function (Eq 4) is based on gradient-descent approaches. The cost function gradient has the  
2 form

$$3 \quad \nabla_{\mathbf{k}} J = \mathbf{B}^{-1}(\mathbf{k} - \mathbf{k}^b) + \sum_{i=1}^l \mathbf{M}_i^T(\mathbf{k}) \nabla_{\mathbf{y}_i} f \quad \text{Eq (5)}$$

4 Where  $\nabla_{\mathbf{k}} J$  and  $\nabla_{\mathbf{y}_i} J$  are the gradients of the cost function  $J$  with respect to  $\mathbf{k}$  and  $\mathbf{y}_i$ , respectively.

5 The expression above allows us to compute  $\nabla_{\mathbf{k}} J$  by knowing  $\nabla_{\mathbf{y}_i} J$ , in the form of a matrix product of this term by the  
6 matrix  $\mathbf{M}_i^T(\mathbf{x}, \mathbf{k})$ , corresponding to the transpose of the Jacobian Matrix. The development of calculation gives the  
7 expression of the gradient of  $\mathbf{y}$  (equation 2):

$$8 \quad \nabla_{\mathbf{k}} J = \mathbf{B}^{-1}(\mathbf{k} - \mathbf{k}^b) + \sum_{i=1}^l \mathbf{M}_i^T(\mathbf{k}) H^T [R_i^{-1}(y_i - y_0)] \quad \text{Eq (6)}$$

9 The control parameters are adjusted several times until a stopping criterion is reached. The iterations of the gradient  
10 method allow us to approach the solution, in order to satisfy a stopping criterion that could be, for example, a certain  
11 threshold on the norm of the cost function gradient.

### 12 3.2 YAO

13 Variational data assimilation requires the computation of the adjoint code of the direct model, which is a heavy and  
14 complex task, especially for a large model such as SECHIBA. Usually, the adjoint code is computed with the help of  
15 specific softwares (automatic differentiators) (e.g., Bischof et al., 1996; Giering and Kaminski, 2003; Hascoët and  
16 Pascual, 2004). These softwares are appropriate for the differentiation of large codes, but their use will be optimal only  
17 under specific coding conventions and a good level of modularity of the codes (Talagrand, 1991). Moreover, manual  
18 optimization of the produced code is often necessary. Therefore, in many practical cases the automatic production of  
19 code will not be totally optimal in terms of flexibility (e.g., when the direct model is updated frequently, one has to  
20 re-differentiate the whole code). These considerations motivated the development of a slightly different but  
21 complementary approach that focuses on the high-level structure of the numerical models, embedding implementation  
22 details inside simple entities that can be easily updated. This has led to the development of the YAO assimilation  
23 software at LOCEAN/IPSL (<https://skyros.locean-ipsl.upmc.fr/~yao/>). YAO is based on the decomposition of a  
24 numerical model into elementary modules interconnected by directional links. On one side, the structure of the model  
25 (variables, dependencies...) is described as a graph structure. On the other side, the details of the physics are coded inside  
26 C/C++ basic modules that are ideally simple. The user can therefore separate the “high-level” structure of the model  
27 from implementation details. It is also very easy to update a numerical code within this framework. Regarding the  
28 assimilation strategy, YAO computes the tangent linear and adjoint codes from the elementary jacobians of each  
29 module (provided by the user). Adjoint/cost function test tools are also available. Finally, YAO includes routines  
30 devoted to classical assimilation scenario (incremental form ...) and is interfaced with the MIQN3 minimizer (Gilbert  
31 and Lemaréchal, 1989).

### 32 3.3 Graph formalism

33 In YAO, a numerical model must be described as an ensemble of modules related by connections in order to form a  
34 graph. Let us define more precisely the main components of the graph:



1 -a **module** is a basic entity of computation, representing a deterministic (but possibly nonlinear) function  
2 transforming an input vector into an output vector. A module is viewed graphically as a node of the graph, the sizes of  
3 the vectors correspond to the number of input and output connections associated with the node.

4 -a **basic connection** is an oriented link relating two nodes of the graph. Most basic connections usually  
5 represent the transmission of the output of one module taken as input by another one.

6 The external context is the ensemble of data input and output points used as external data by a whole graph at a  
7 specific level of abstraction. Basic connections link a data input point located in the external context to one or  
8 several module(s) (for instance modules needing the specification of some initial conditions, boundary conditions or  
9 model parameters). Inversely, the global outputs of the model link a module towards a data output point located in the  
10 external context.

11 The modular graph is the ensemble of the modules and of their connections. It must be acyclic so that a  
12 topological order may be defined on the nodes of the graph (i.e., if there is connection  $F_p \rightarrow F_q$ , then  $F_p$  should be  
13 computed before  $F_q$ ) (see Fig.1)

14

15 Typically, a modular graph describes the equations governing the system of interest and each physical variable appearing  
16 in the governing equations are associated with a specific module. However, supplementary modules can also be defined  
17 to represent temporary variables required to simplify computations for complex equations. The user has generally to  
18 specify modules at a single point  $(i, j, k, t)$  of space  $(i, j, k)$  and time  $(t)$ , and the names and space-time locations (e.g.  $i+1$ ,  
19  $j-1, k, t-1$ ) of the discretized variables taken as inputs. From the local description of the equations, YAO is able to build a  
20 model on a given space domain and on a given number of time steps by automatically replicating the local graph in  
21 space-time (cf. Fig.2)).

22 By passing the different modules in topological order, YAO is clearly able to emulate the global model and to  
23 calculate the global model outputs given model initial conditions and parameters.

24 Now, we will see that the usefulness of the graph modular approach is reinforced when the jacobian matrix of each basic  
25 function is known. For a basic function  $F$  such that  $y = F(x)$ , the jacobian matrix  $F$  relates a perturbation of the inputs to  
26 the associated perturbation of outputs:  $dy = F dx$ . Since the jacobian of a composition of functions is the product of the  
27 elementary jacobians, the tangent linear model associated with a modular graph may also be obtained by passing the  
28 graph in the same topological order.

29 The “lin-forward” algorithm is the following:

30 1) Initialize the external context data input points with a perturbation  $dx_i$  (around a given linearization point)

31 2) Pass the modules in topological order and propagate the perturbation

32

33 3) Estimate the perturbation output  $dy$  on output data points in the external context of the graph.

34 Following this procedure, YAO can emulate the global tangent-linear model from elementary jacobians. In the same  
35 manner, a backward algorithm may be defined for adjoint computations. From (Eq. 1), it may be shown that the global  
36 adjoint will be retrieved by back-propagating the graph, with a few adjustments not detailed here (see, Nardi et al., 2009  
37 for more details on the “backward” algorithm). This property is the basis of the semi-automatic adjoint computation by  
38 YAO.

39 An implementation of a variational assimilation procedure with YAO follows the structure represented in Fig. 3. The  
40 YAO compiler builds an executable file following the scheme presented in Fig.3. This file is independent of the



1 assimilation instructions. The executable file reads these instructions when the user calls them. However, it is not  
2 compulsory to use an instruction file since YAO accepts a command-line instruction if no instruction file is provided.  
3 Due to the graph structure of the model and of its adjoint, it is easy to modify the model and its adjoint, e.g. by  
4 updating some adequate modules; one can systematically obtain the update global direct model and the global adjoint  
5 As mentioned in the introduction, this paper gives access to a compiled version of SECHIBA-YAO and allows to  
6 perform some assimilation experiments related to the control of the ten most influent internal parameters of SECHIBA by  
7 observing the land surface temperature. YAO is a free software that gives the opportunity to modify the SECHIBA code  
8 provided in this paper.

### 9 **3.4 Development of SECHIBA-YAO**

10 The implementation of SECHIBA in YAO starts with the definition of the modular graph describing the dynamics of the  
11 model (see ANNEX A). Elementary processes and interconnections between modules are defined in order to catch the  
12 essence of the model. The modular graph is the basis of all the integration processes made by YAO. Direct and adjoint  
13 models are computed following the modular graph structure. The modular graph was built as follows:

- 14 -Every component of the original code was carefully studied line by line directly.
- 15 -A list of inputs and outputs for each subroutine was made, for every routine of SECHIBA. This permits to exactly know  
16 the information flow in the model.
- 17 -A second zoom in the subroutines was made in order to understand the internal dynamics of the code. This is the last  
18 step in the modular graph definition. When studying the subroutines, they were very general and a division into simpler  
19 elements was inevitable, with the purpose of reducing the coupling and increasing the cohesion of the modules. The idea  
20 is to have a scalable code. Uncoupled modules give more independence when changing part of the model. Cohesive  
21 modules help to understand the model.
- 22 -The original six subroutines in the SECHIBA-Fortran code are split into 130 modules by the SECHIBA-YAO modular  
23 graph, corresponding to every process modeled by SECHIBA and to a number of transitional modules serving as  
24 auxiliary computing.
- 25 -It is important to mention that every variable and subroutine name was kept as in the original model. If a user or  
26 developer of SECHIBA-Fortran sees the implementation in YAO, he will find his way easily.

#### 27 **3.4.1 Direct model**

28 After defining the modular graph in YAO, the second step in the SECHIBA-YAO implementation is the coding of the  
29 direct and the derivatives of the modules. This consists in coding the different modules directly with YAO meta-  
30 language. Every module is represented as a script and the different processes attributed to the module are implemented  
31 inside the script, allowing a better control of the physics, i.e. any change in the physics could be made easily. In  
32 SECHIBA-YAO, the second approach was used.

#### 33 **3.4.2 Module Derivatives**

34 Once the direct model has been coded and validated, there are two options to code the derivatives: they can be coded  
35 line-by-line based on the forward computing, in order to obtain the Jacobian matrix of the module, or they can also be  
36 produced routinely, using an automatic differentiation tool (for example, Tapenade (Hascoët et al, 2012)). For  
37 SECHIBA-YAO, the derivative process was made line-by-line. The outputs are derived with respect to every input. YAO  
38 generates automatically, based on these derivatives, the tangent linear and the adjoint of the model.





1 Nevertheless, the derivative process introduced errors related to the coding process, to inexact derivatives, expressions  
2 that were not differentiated among others. In order to reduce it to a minimum number of bugs, the adjoint of the model  
3 was validated (as it was made with the direct model). This guarantees the accuracy when performing assimilation. The  
4 validation of the adjoint model is presented in section 4. More validations of the direct and the adjoint models are  
5 available in Benavides, 2014.

#### 6 **4. Data assimilation experiments**

7 In this section we present several experiments that have been realized using the SECHIBA-YAO. They are related to the  
8 control of the eleven most influent internal parameters of SECHIBA by observing the land surface temperature.

9 The parameters are divided into two groups: inner parameters and multiplying factors (Table 1). The first group  
10 corresponds to physical parameters. The second group collects parameters weighting some physical processes of  
11 SECHIBA. In the initial model, they are all normalized to 1 indicating that no weights are used, thus the effect of the  
12 assimilation is to allow a local adaptation of these weighting factors. The model inner parameters are the following:  
13  $rsol_{cste}$  is a numerical constant involved in the soil resistance to evaporation. This parameter limits the soil evaporation, so  
14 the greater its value the lower the evaporation;  $hum_{cste}$ ,  $mx_{eau}$  and  $min_{drain}$  are related to soil water processes, the higher  
15 their values, the more water will be available in the model reservoir, affecting water transfers and especially  
16 evapotranspiration;  $dpu_{cste}$  represents the soil depth in meters. The other parameters are multiplicative factors. We have  
17  $k_{rveg}$  which is used in the calculation of the stomatal resistance, this variable limits the transpiration capacity of leaves, the  
18 greater its value, the lower the transpiration;  $k_{emis}$  controls the soil emissivity used to compute land surface temperature.  
19 This parameter takes part in the net radiation calculation which determines the energy balance between incoming and  
20 outgoing surface fluxes;  $k_{albedo}$  weights the surface albedo, which is defined as the reflection coefficient for short wave  
21 radiation;  $k_{cond}$  and  $k_{capa}$  take part in the thermal soil capacity and conductivity, both involved in the computation of the  
22 soil thermodynamics and  $k_{z0}$  weights the roughness height, which determines the surface turbulent fluxes. The control  
23 parameters are normalized from their prior value, so their optimal value is always equal to 1 and thus, only relative  
24 perturbations are considered. If the control parameter values posterior to the assimilation process are close to 1, it means  
25 that the parameter prior values were retrieved successfully. Differences between the values retrieved and the prior values  
26 represent relative errors on the parameter estimation, posterior to assimilation.

27 Prior to the assimilation process, different scenarios were defined for the tests. A scenario makes reference to the  
28 experimental conditions. It includes the definition of the vegetation functioning type (PFT), the type of observation to be  
29 assimilated, the observation sampling, the time sampling, and the atmospheric forcing file, the subset of control  
30 parameters, the assimilation window size and the time of the year to start the assimilation. The different scenarios were  
31 calculated using the adjoint model for several typical summer conditions of the two Fluxnet sites selected. The dates  
32 presented in this paper are representative of sunny days in summer or winter, with no perturbation coming from clouds  
33 and without rainfall events. In order to show the benefit of data assimilation in SECHIBA, we conducted several  
34 experiments using SECHIBA-YAO. The next section explains the scenarios for the different experiments performed in  
35 this work.

#### 36 **4.1 Variational sensitivity analysis**

37 In order to show the accuracy of the distributed SECHIBA-YAO code, we present an analysis that allows to rank the  
38 eleven parameters according to their sensibility estimated by using the adjoint model and to compare the results to those  
39 obtained by using finite differences. We identify the most sensitive parameters to the estimation of land surface



1 temperature by computing the gradients obtained with the adjoint model. This analysis corresponds to a first-order  
 2 sensitivity estimate of the influence of the control parameters on the land surface temperature. In order to do so, local  
 3 sensitivities were computed, providing the slope of the calculated model output variations in the parameter space for a  
 4 given set of values (Saltelli et al, 2008). This method is really local and the information provided is related to a definite  
 5 point in the parameter space. The values of the 11 parameters concerned in the analysis are presented in Table 1, they  
 6 represent the initial values where the experiments have been conducted. Although  $hum_{cste}$  is related to vegetation type, in  
 7 this work only value for PFT 1 ( $5\text{ m}^{-1}$ ) and PFT 12 ( $2\text{ m}^{-1}$ ) are considered.

8 The sensitivity analysis was performed for a subset of inner parameters related to the energy and water physical  
 9 processes on bare soil (PFT 1) and agricultural C3 crop (PFT 12), in order to quantify the role of the vegetation on the  
 10 land surface temperature parameters' sensitivity. The work was made on a daily basis, in order to observe the diurnal  
 11 variations of sensitivities. At each half-hour time step, the model is restarted. At each time step, a gradient is computed in  
 12 order to have the updated gradient value. Since no prior values of the control parameters is known, as mentioned in  
 13 section 2, there is no background and the initial values of the parameters are those of Table 1. We recall that for  
 14 numerical purpose, the control parameters have been normalized in order to have the same order of magnitude (i.e. equal  
 15 to 1) during the minimization process.

16 Figure 4 compares, for August 26, 1996 at Harvard Forest, the sensitivities computed for each control parameter with  
 17 both finite differences and model gradients. Bare soil results are presented in Fig.4(a). The agricultural C3 crop scenario  
 18 is illustrated in Fig.4(b). The efficiency of the adjoint calculation is first demonstrated in these plots, because the 11  
 19 desired parameters sensitivities are obtained in a single integration. By using the same methodology, sensitivity curves  
 20 were computed in the Fluxnet site Kruger Park, which are presented in Benavides (2014)

21 The comparison between sensitivity analysis done using the adjoint and using finite differences shows a very good  
 22 agreement between the two methods (the same results, not shown, were obtained with the Kruger Park site). For more  
 23 information, consult Benavides (2014), where the comparison between the two approaches is developed. The diurnal  
 24 characteristics of the parameter sensitivities with a maximum around noon in phase with the diurnal variation of solar  
 25 radiation are clearly visible.

26 Table 2 presents, for Harvard Forest and Kruger Park, the 11 parameters ranked with respect to their influence.  
 27 According to the four scenarios defined (two sites and two PFT), it can be seen that the hierarchy change with the  
 28 vegetation, but remains the same for both sites. Parameter hierarchy revealed that the highest gradient values correspond  
 29 to those that have the largest influence on the land surface temperature estimate. Clearly  $k_{emis}$  is the most influential  
 30 parameter in the calculation of land surface temperature, regardless of the climatology used and vegetation fraction. In  
 31 addition,  $min_{drain}$  is the least influential parameter for all scenarios.

32 The parameters  $k_{capa}$ ,  $k_{cond}$ ,  $k_{z0}$  and  $k_{albedo}$  are the most influential in bare soil conditions, after  $k_{emis}$ . In the presence of  
 33 vegetation, several sensitivities change radically:  $k_{rveg}$  becomes the most important multiplicative factor after  $k_{emis}$ ; the  
 34 factor  $k_{albedo}$  is less sensitive compared to its influence in the bare soil case and  $mx_{eau}$  is more sensitive, given that less  
 35 water is available when a fraction of vegetation is present. The other parameters show equivalent sensitivity values  
 36 regardless the scenario. For  $hum_{cste}$  and  $k_{rveg}$ , sensitivities are equal to zero for bare soil, because these parameters affect  
 37 surface temperature only in presence of vegetation.

38 Parameters with persistent positive sensitivity are:  $rsol_{cste}$ ,  $k_{rveg}$  and  $hum_{cste}$ . Parameters with persistent negative  
 39 sensitivity are:  $k_{z0}$ ,  $k_{albedo}$  and  $emis$ . The sign of the gradients reflects the positive or negative feedback on the surface  
 40 temperature of the processes involved. For example, the parameters involved in the evapotranspiration processes present



1 negative sensitivities because a reduction (respectively an increase) of the evapotranspiration will lead to an increase  
2 (respectively a decrease) of the land surface temperature, when the soil water content is sufficient.  
3 Transpiration processes influence directly the land surface temperature in presence of vegetation and is the dominant  
4 process in the studied sites. Therefore  $k_{rveg}$  has a higher sensitivity than  $k_{cond}$ ,  $k_{capa}$  and  $k_{albedo}$ . For bare soil, on the  
5 contrary, the dominant processes are those related to the soil thermodynamics, explaining why  $k_{capa}$ ,  $k_{cond}$  and  $k_{emis}$  are the  
6 most sensitive parameters.  
7 In general, sensitivities are higher in bare soil conditions for the control parameters, except for  $min_{drain}$  and  $mx_{eau}$ . Since  
8  $min_{drain}$  is not sensitive to the land surface temperature, this parameter is no longer controlled. Only the ten most influent  
9 parameters are used in the following sections.  
10 The next section presents the different assimilation experiments that can be performed using the SECHIBA-YAO  
11 software.

## 12 4.2 Twin experiments

13 Twin experiments are synthetic tests checking the robustness of the variational assimilation method. The model is run  
14 with a set of parameters or initial conditions ***Ptrue*** in order to produce pseudo observations of land surface temperature  
15 ***Tobs***. Then ***Ptrue*** is randomly noised to obtain ***Pnoise***. Assimilations of land surface temperature ***Tobs*** were then  
16 performed in the model forced with ***Pnoise*** during several days (most of the time, one week), leading to a new set of  
17 optimized parameters denoted ***Passim***. Three different assimilation experiments were performed. These experiments are  
18 available in the distributed version of SECHIBA-YAO.

## 19 4.3 Experiment Definition

20 The 10 most sensitive parameters are considered in the twin experiments (all parameters except  $min_{drain}$ ). We present here  
21 the results obtained for one particular random perturbation of the parameters (the one provided in the distributed version,  
22 see Section 5). A statistic made with 500 different random realizations gave the same performances (Benavides, 2014).  
23 Each experiment was perturbed with a uniform distribution random noise reaching 50% of the parameter nominal value.  
24 We ran the assimilations in each experiment by randomly perturbing the initial conditions presented in Table 1. This  
25 permitted us to obtain the relative errors of the control parameters and the relative values of the root mean square error  
26 (RMSE) of the model flux, based on their value before and after the assimilation process. The fluxes considered are the  
27 land surface temperature ( $LST$ ), the sensible ( $H$ ) and latent heat ( $LE$ ).

28 Scenarios for all the assimilation experiments are presented in Table 3. All parameters are controlled at the same time.  
29 The duration of each assimilation experiment is one week and the time increment  $\Delta T$  is 30 minutes. All experiments  
30 presented in this work use Harvard Forest as forcing. Same experiments are developed for Kruger Park site in Benavides  
31 (2014).

32 In Experiment 1 the five most sensitive parameters are controlled in bare soil conditions, according to the sensitivity  
33 analysis (Table 2), during one week in Harvard Forest site.

34 In Experiment 2 the five most sensitive parameters are controlled in conditions of agricultural C3 (PFT 12), according to  
35 the sensitivity analysis (Table 2), in Harvard Forest site during a week.

36 With these two experiments, we are able to assess the effect of the vegetation fraction on the assimilation system. In  
37 addition, taking only the most sensitive parameters in the control set permitted to increase the assimilation performances,



1 given that the more the observed variable is sensitive to a parameter, the easier the minimization process finds its optimal  
2 value, and consequently reducing the estimation error.

3 In Experiment 3, all parameters, except  $min_{drain}$ , are controlled (since  $min_{drain}$  has no impact in the land surface  
4 temperature estimation), during a week in Harvard Forest.

5 Comparing Experiment 3 with Experiments 1 and 2 allows us to study the impact of taking a larger control parameter set  
6 in the assimilation process. In addition, we want to test if land surface temperature as observation, provides enough  
7 information to constrain all the model parameters at the same time and if we can hope to improve all model state  
8 variables.

#### 9 4.4 Results

10 The RMSE errors of the assimilations for experiments 1, 2 and 3 are presented in Table 4 (resp Table 5) corresponding to  
11 Harvard Forest site.

12 In Experiment 1, the errors on the retrieved values for all the control parameters are of the order of  $10^{-8}$ . Regarding the  
13 land surface temperature, the RMSE ranges from 4.82 K prior assimilation, decreasing to  $2.1 \cdot 10^{-5}$  K after the assimilation  
14 process. Same behavior is observed for the different model fluxes. Experiment 2 yields similar results as in Experiment 1.  
15 The assimilation process allows the reduction of the parameter errors (Fig.5 and Fig.6).

16 Relative value of the RMSE, with respect to the synthetic measurements, for  $LST$ ,  $LE$  and  $H$  in Experiment 3 prior to  
17 assimilation, are equal to 3.12 K,  $34.1 \text{ W/m}^2$  and  $30.4 \text{ W/m}^2$ , respectively. After assimilation, the RMSE is reduced for  
18 both sites. The same holds for the mean relative error of the control parameters.

19 Comparing the results from Experiments 1 and 2 to Experiment 3, degradation in fluxes and parameter restitution can be  
20 observed. Effectively, we find higher errors in the fluxes and the final control parameters when increasing the size of the  
21 control parameter set (Experiment 3). Best performances in the parameters restitution are always for the control of 5  
22 parameters. When we control the 10 most sensitive parameters, as in Experiment 3, degradation in the final value of the  
23 parameters is observed. This can be explained by the complexity of the model, the larger the control parameters set, the  
24 more difficult it is to find local minima that correspond to the initial control parameters values used to produce the  
25 synthetic observations. It is difficult to retrieved parameters that are insensitive to LST, thus the assimilation of this  
26 variable in order to optimize these parameters is not optimal.

#### 27 5. Conclusion

28 In this study the adjoint of SECHIBA was implemented, using an adjoint semi-generator software denoted YAO. With  
29 SECHIBA-YAO, land surface temperature gradients with respect to each control parameter were computed, with the aim  
30 at carrying out a sensitivity analysis of the parameter influence on LST estimation.

31 The first contribution of this paper is the sensitivity analysis results. They show exactly which parameters of the model  
32 are the most sensitive and have to be controlled during the assimilation process. However, it is important to mention that  
33 sensitivity analysis depends on the region, the forcing, the PFT, the time period (hour and day), among other factors.  
34 Once the parameter hierarchy was set, twin experiments were performed for different scenarios, aiming at testing the  
35 robustness of the assimilation scheme.

36 The second contribution of this work is that we showed the usefulness of the variational data assimilation of LST to  
37 improve SECHIBA parameter estimations. Land surface temperature assimilation has the potential of improving the  
38 LSM parameter calibration, by adjusting properly the control parameters. In a forecasting approach, this can be valuable,  
39 given that simulation can be more reliable since they are fitted on actual measurements. The improvement in the model



1 fluxes after the assimilation of LST was demonstrated. Twin experiments showed the power of variational data  
2 assimilation to improve model parameter estimation. For different scenarios and forcing sites, the different experiments  
3 were successfully accomplished, meaning that a reduction in the fluxes errors was obtained by introducing information  
4 given by the LST synthetic observations. In addition, the influence that the size of the control parameter set has in the  
5 assimilation performance was shown.

6 Adding extra parameters to the control set increases the complexity of the cost function. Taking into consideration the  
7 results of assimilation of land surface temperature when controlling the 10 most sensitive parameters (Experiment 3), we  
8 can see that, after having made several assimilation runs, land surface temperature does not provide enough information  
9 to constrain the parameter set, in order to improve the estimation of state variables in SECHIBA. In the case of  
10 controlling all parameters we cannot hope improving all model state variables unless we assimilate additional  
11 observations.

12 Assimilation with the YAO approach permits the implementation of different assimilation scenarios in a very flexible  
13 way, when performing different twin experiments: the control parameters and the observed variables (once the adjoint  
14 code has been generated), the assimilation windows, the observation sampling, the time sampling and other different  
15 features can be changed easily.

16 A distributed version of SECHIBA-YAO code and several examples with different scenarios are available at a GitHub  
17 dedicated site. YAO can be downloaded upon request at <https://skyros.locean-ipsl.upmc.fr/~yao/>. Direct use of this  
18 software will allow performing other experiments using different physical conditions or even changing several equations  
19 of the model.

## 20 **6. Code and data availability**

21 The distributed version of SECHIBA-YAO provides an opportunity for scientists to perform their own assimilation. The  
22 distributed version allows the control of the 5 most influent internal parameters of SECHIBA, depending on the  
23 vegetation type. In addition, LST or satellite brightness temperature can be used as observations.

24 The distributed version of SECHIBA-YAO is available in a GitHub repository  
25 (<https://github.com/brajard/sechibavar/archive/v1.0.zip>), the user can download the software, save it in a local repertory  
26 and run the *makefile* in order to build a local executable. Documentation and two instruction files are available in order to  
27 guide the user towards their own implementation. Users can modify the forcing file, the initial date to the assimilation,  
28 the parameters value and their perturbation if needed. The assimilation frame (1 week), the step time (30 minutes), the  
29 observed variable (land surface temperature), the control parameters (only 5) and other initial parameters are imposed. If  
30 user wants to have access to a full modifiable version, YAO software has to be installed ([https://skyros.locean-  
31 ipsl.upmc.fr/~yao/](https://skyros.locean-ipsl.upmc.fr/~yao/)).

32 The instructions files given with the distributed version correspond to the twin experiments presented in this paper  
33 (Experiments 1 and 2). Initial parameters like the assimilation time frame and the observed variable (LST) cannot be  
34 changed in the distributed version. However the other initial parameters used to build different scenarios can be changed  
35 easily through the instruction file (initial parameter values, PFT, observations files, forcing, initial date, etc).

## 36 **Acknowledgements**

37 This work used eddy covariance data acquired by the FLUXNET community and in particular by the following networks:  
38 AmeriFlux (U.S. Department of Energy, Biological and Environmental Research, Terrestrial Carbon Program and  
39 AfriFlux). Dr. P. Peylin, F. Chevalier and M. Crépon are acknowledged for fruitful discussions. We thank also Dr. F.



1 Maignan for its continuous support in the use of ORCHIDEE model, and Dr. M. Berrondo, for the assistance in writing  
 2 this article.

### 3 **7. References**

- 4 Aubinet, M., Vesala, T., Papale, D. Eddy. Covariance: A Practical Guide to Measurement and Data Analysis. Springer  
 5 Atmospheric Sciences Editions, United States of America. 2012.
- 6 Baldocchi, D., Falge, E., Gu, L., Olson, R., Hollinger, D., Running, S., Anthoni, P., Bernhofer, C., Davis, K., Evans, R.,  
 7 Fuentes, J., Goldstein, A., Katul, G., Law, B., Lee, X., Malhi, Y., Meyers, T., Munger, W., Oechel, W., Paw, K. T.,  
 8 Pilegaard, K., Schmid, H. P., Valentini, R., Verma, S., Vesala, T., Wilson, K., Wofsy, S. FLUXNET: a new tool to study  
 9 the temporal and spatial variability of ecosystem-scale carbon dioxide, water vapor, and energy flux densities. *Bull. Am.*  
 10 *Meteorol. Soc.*, 82, 2415–2434. 2001
- 11 Barrett, D., Renzullo, L. On the Efficacy of Combining Thermal and Microwave Satellite Data as Observational  
 12 Constraints for Root-Zone Soil Moisture Estimation. CSIRO Land and Water, 1109-1127, Canberra, Australia. 2009.
- 13 Bateni, S.M., Entekhabi, D., Jeng, D.S. Variational assimilation of land surface temperature and the estimation of surface  
 14 energy balance components. *Journal of Hydrology*, 481,143–156. 2013.
- 15 Hector Simon Benavides Pinjosovsky. Variational data assimilation in the land surface model ORCHIDEE using YAO.  
 16 Earth Sciences. Université Pierre et Marie Curie - Paris VI, 2014. English. <NNT : 2014PA066590>. <tel-01145923>.  
 17 Available at <http://www.theses.fr/2014PA066590>
- 18 Castelli F., Entekhabi, D., Caporali, E. Estimation of surface heat flux and an index of soil moisture using adjoint-state  
 19 surface energy balance. *Water Resources Research*, 35, 10, 3115-3125. 1999.
- 20 d’Orgeval, T., Polcher, J., and Li, L. Uncertainties in modelling future hydrological change over west africa. *Climate*  
 21 *Dynamics*, 26, 93–108. 2006.
- 22 Ducoudré, N., Laval, K., and Perrier, A. SECHIBA, a new set of parametrizations of the hydrologic exchanges at the  
 23 land/atmosphere interface within the LMD atmospheric general circulation model. *J. Climate*, 6, 248–273. 1993.
- 24 Evensen, G. The ensemble Kalman filter: Theoretical formulation and practical implementation. *Ocean Dyn.*, 53, 343–  
 25 367. 2003.
- 26 Friedlingstein P., Joel G., Field C. B., Fung I. Toward an allocation scheme for global terrestrial carbon models. *Global*  
 27 *Change Biology*, 5, 755-770. 1999.
- 28 Ghent, D., Kaduk, J., Remedios, J. and Balzter, H. Data assimilation into land surface models: The implications for  
 29 climate feedbacks. *International Journal of Remote Sensing*, 3, 617 — 632. 2011.
- 30 Giering, R., Kaminski., T. Recipes for Adjoint Code Construction. *ACM Transactions on Mathematical Software*, 24,  
 31 437–474. 1998.
- 32 Gilbert, J.C., LeMaréchal, C. Some numerical experiments with variable-storage quasi Newton algorithms, *Maths.*  
 33 *Program*, 45, 407-435. 1989.
- 34 Harrison, D.E., Chiodi A.M, Vecchi, G.A.Effects of surface forcing on the seasonal cycle of the eastern equatorial Pacific.  
 35 *J. Mar. Res.* 67, 701-729. 2009.
- 36 F. Hourdin, I. Musat, S. Bony, P. Braconnot, F. Codron, J.-L. Dufresne, L. Fairhead, M.-A. Filiberti, P. Friedlingstein, J.-  
 37 Y. Grandpeix, G. Krinner, P. LeVan, Z.-X. Li et F. Lott, 2006, The LMDZ4 general circulation model : climate  
 38 performance and sensitivity to parametrized physics with emphasis on tropical convection,  
 39 *Climate Dynamics*, 27 : 787-813



- 1 Huang, C., Li, X., Lu, L. Retrieving land surface temperature profile by assimilating MODIS LST products with  
2 ensemble Kalman filter. Cold and Arid Regions Environmental and Engineering Research Institute, CAS, Lanzhou,  
3 China. 2003.
- 4 Ide, K., Courtier, P., Ghil, M. et Lorenc, A. Unified Notation for Data Assimilation : Operational, Sequential and  
5 Variational. Special Issue J. Meteorological Society Japan, 75, 181–189. 1997.
- 6 Krinner, G., Viovy, N., Noblet-Ducoudre, N. de, Ogee, J., Polcher, J., Friedlingstein, P.,  
7 Ciais, P., Sitch, S., and Prentice, I. C. A dynamic global vegetation model for studies of  
8 the coupled atmosphere-biosphere system. *Global Biogeochem. Cycles*, 19. 2005.
- 9 Kuppel, S., Peylin, P., Chevallier, F., Bacour, C., Maignan, F. and Richardson, A. Constraining a global ecosystem model  
10 with multi-site eddy-covariance data. *Biogeosciences*, 9, 3757–3776. 2012.
- 11 Lahoz, W; Khattatov, B. *Data Assimilation Making Sense of Observations*. Springer Editions. 2010.
- 12 Le Dimet, F.-X., Talagrand, O. *Variational Algorithms for Analysis and Assimilation of Meteorological Observations:  
13 Theoretical Aspects*. *Dynamic Meteorology and Oceanography* 38. 1986.
- 14 Nardi, L., Sorrow, C., Badran, F., and Thiria, S. YAO: A Software for Variational Data Assimilation Using Numerical  
15 Models. *Computational Science and its Applications - ICCSA 2009. International Conference*, 5593, 2, 621-636. 2009.
- 16 Pipunic, R. C., Walker, J. P., and Western, A. Assimilation of remotely sensed data for improved latent and sensible heat  
17 flux prediction: A comparative synthetic study. 19<sup>th</sup> International Congress on Modelling and Simulation, Perth,  
18 Australia. 2008.
- 19 Reichle, R., Walker, J., Koster, R., Houser, P. Extended versus Ensemble Kalman Filtering for Land Data Assimilation.  
20 *Journal of Hydrometeorology*, 3, 728-740. 2001.
- 21 Reichle, R., Kumar, S., Mahanama, S., Koster, R. D., and Liu, Q. Assimilation of satellite-derived skin temperature  
22 observations into land surface models. *Journal of Hydrometeorology*, 11, 1103-1122. 2010.
- 23 Ridler, M., Sandholt, I., Butts, M., Lerer, S., Mougin, E., Timouk, F., Kergoat, L., Madsen, H. Calibrating a soil–  
24 vegetation–atmosphere transfer model with remote sensing estimates of surface temperature and soil surface moisture in  
25 a semi-arid environment. *Journal of Hydrology* 436–437, 1–12. 2012.
- 26 Robert, C, Blayo, E., Verron, J. Comparison of reduced-order, sequential and variational data assimilation methods in the  
27 tropical Pacific Ocean. *Ocean Dynamics* 56, 5-6 (2006) 624-633. 2007
- 28 Saltelli, A. *Sensitivity Analysis*. John Wiley & Sons Edition. United States of America. 2008
- 29 Sitch, S., Smith, B., Prentice, I.C., Arneth, A., Bondeau, A., Cramer, W., Kaplan, J.O., Levis, S., Lucht, W., Sykes, M.T.,  
30 Thonicke, K., Venevsky, S. Evaluation of ecosystem dynamics, plant geography and terrestrial carbon cycling in the LPJ  
31 dynamic global vegetation model. *Glob. Change Biol.* 9, 161 –185. 2003.
- 32



1

Parameter	Description	Prior Value	Unit
<b>Inner Parameters</b>			
hum <sub>cste</sub>	Water stress	{5, 2}	m <sup>-1</sup>
rsol <sub>cste</sub>	Evaporation resistance	33000	S/m <sup>2</sup>
mindrain	Diffusion between reservoirs	0,001	-
dpu <sub>cste</sub>	Total depth of soil water pool	2	m
mX <sub>eau</sub>	Maximum water content	150	Kg/m <sup>3</sup>
<b>Multiplying Factors</b>			
k <sub>emis</sub>	Surface Emissivity	1	-
k <sub>capa</sub>	Soil Capacity	1	-
k <sub>cond</sub>	Soil Conductivity	1	-
k <sub>rveg</sub>	Vegetation Resistant	1	-
k <sub>z0</sub>	Roughness height	1	-
k <sub>albedo</sub>	Surface albedo	1	-

2

3 Table 1. SECHIBA Parameters studied in this work. There are 6 inner parameters, involved in the model estimations and  
4 5 multiplying factors that are imposed to specific fluxes

5





1

Site	Bare Soil (PFT 1)	Agricultural C3 crop (PFT 12)
Harvard Forest	$k_{emis}$ , $k_{cond}$ , $k_{capa}$ , $k_{z0}$ , $k_{albedo}$ , $dpu_{cste}$ , $rsol_{cste}$ , $mx_{eau}$ $min_{drain}$ , $k_{rveg}$ , $hum_{cste}$	$k_{emis}$ , $k_{rveg}$ , $k_{cond}$ , $k_{capa}$ , $k_{z0}$ , $mx_{eau}$ , $hum_{cste}$ , $k_{albedo}$ , $dpu_{cste}$ , $rsol_{cste}$ , $min_{drain}$
Kruger Park	$k_{emis}$ , $k_{cond}$ , $k_{capa}$ , $k_{z0}$ , $k_{albedo}$ , $dpu_{cste}$ , $rsol_{cste}$ , $mx_{eau}$ $min_{drain}$ , $k_{rveg}$ , $hum_{cste}$	$k_{emis}$ , $k_{rveg}$ , $k_{cond}$ , $k_{capa}$ , $k_{z0}$ , $mx_{eau}$ , $hum_{cste}$ , $k_{albedo}$ , $dpu_{cste}$ , $rsol_{cste}$ , $min_{drain}$

2

3 Table 2. Sensitivity analysis result. Parameter hierarchy according to each site and vegetation fraction.



1

Conditions	Experiment 1	Experiment 2	Experiment 3
<b>Assimilation period</b>	3 Mars 1996, (Harvard Forest)	3 Mars 1996 1 week (Harvard Forest)	8 August 1996, 1 week (Harvard Forest)
<b>Control Parameters</b>	$k_{emis}$ , $k_{cond}$ , $k_{capa}$ , $k_{z0}$ , $k_{albedo}$	$k_{emis}$ , $k_{rveg}$ , $k_{cond}$ , $k_{capa}$ , $k_{z0}$	All parameters, except $min_{drain}$
<b>Observations</b>	Land surface temperature	Land surface temperature	Land surface temperature
<b>Observation sampling</b>	30 minutes	30 minutes	30 minutes
<b>Vegetation type</b>	PFT 1 (Bare Soil)	PFT 12 (Agricultural C3crop)	PFT 12 (Agricultural C3crop)

2

3 Table 3. Scenarios for each of the 3 twin experiments

4



1

	Experiment 1 (PFT 1)				Experiment 2 (PFT 12)			
	Relative error (%)		RMSE		Relative error (%)		RMSE	
	Prior	Final	Prior	Final	Prior	Final	Prior	Final
LST (K)	5.2	$3.1 \cdot 10^{-10}$	4.82 K	$2.1 \cdot 10^{-5}$ K	7.78	$1.35 \cdot 10^{-6}$	1.61 K	$1.10^{-10}$ K
LE(W/m <sup>2</sup> )	5.10	$5.1 \cdot 10^{-6}$	2.5 W/m <sup>2</sup>	$6.6 \cdot 10^{-4}$ W/m <sup>2</sup>	13.56	$1.2 \cdot 10^{-5}$	8.52 W/m <sup>2</sup>	$1.2 \cdot 10^{-6}$ W/m <sup>2</sup>
H(W/m <sup>2</sup> )	2.53	$1.59 \cdot 10^{-8}$	2.03 W/m <sup>2</sup>	$1.1^{-12}$ W/m <sup>2</sup>	39.23	$1.3 \cdot 10^{-3}$	1.39 W/m <sup>2</sup>	$1.2 \cdot 10^{-10}$ W/m <sup>2</sup>

(a)

2

	Relative error (%)			
	Experiment 1 (PFT 1)		Experiment 2 (PFT 12)	
	Prior	Final	Prior	Final
$k_{\text{emis}}$	14.69	0	20.92	$5.019 \cdot 10^{-3}$
$k_{g0}$	28.18	0	48.42	$6.81 \cdot 10^{-3}$
$k_{\text{cond}}$	44.99	0	38.8	$3.23 \cdot 10^{-3}$
$k_{\text{capa}}$	48.98	0	11.48	$7.32 \cdot 10^{-3}$
$k_{\text{rveg}}$	-	-	44.83	$1.69 \cdot 10^{-3}$
$k_{\text{albedo}}$	38.25	$2.384 \cdot 10^{-7}$	-	-

(b)

3

4

5 Table 4. Results for Experiments 1 (PFT 1) and 2 (PFT 12). RMSE of model fluxes (a) and Parameters Relative errors (b)  
 6 before and after the assimilation process on FLUXNET Harvard Forest, 03 Mars 1996 during a week



1

Experiment 3 (PFT 12)				
	Relative error (%)		RMSE	
	Prior	Final	Prior	Final
LST (K)	5.12	$1.1 \cdot 10^{-3}$	3.12 K	$3.2 \cdot 10^{-1}$ K
LE(W/m <sup>2</sup> )	7.10	$5.2 \cdot 10^{-2}$	34.1 W/m <sup>2</sup>	3.1 W/m <sup>2</sup>
H(W/m <sup>2</sup> )	2.53	$2.39 \cdot 10^{-2}$	30.4 W/m <sup>2</sup>	2.1 W/m <sup>2</sup>

2

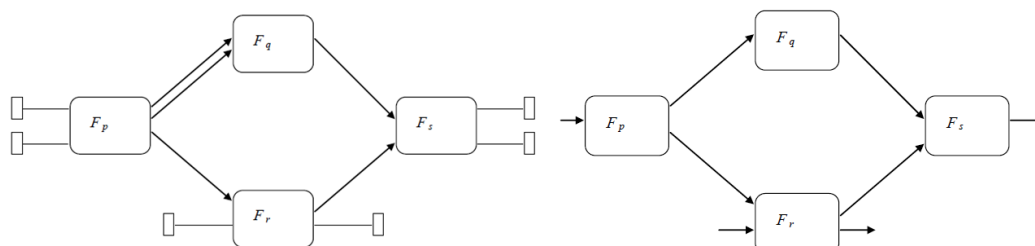
(a)

Relative error (%) (PFT 12)		
Experiment 3		
	Prior	Final
$k_{emis}$	26.3	$2.1 \cdot 10^{-1}$
$k_{z0}$	25.4	$1.79 \cdot 10^{-1}$
$k_{cond}$	25.1	$3.30 \cdot 10^{-1}$
$k_{capa}$	26.7	$2.61 \cdot 10^{-1}$
$k_{rveg}$	27.5	$2.8 \cdot 10^{-1}$
$k_{albedo}$	24.7	$2.37 \cdot 10^{-1}$
$m_{x_{eau}}$	25.8	$7.34 \cdot 10^{-1}$
$hum_{este}$	25.2	$2.7 \cdot 10^{-1}$
$dpu_{este}$	24.2	$2.2 \cdot 10^{-1}$
$rsol_{este}$	25.4	$2.36 \cdot 10^{-1}$

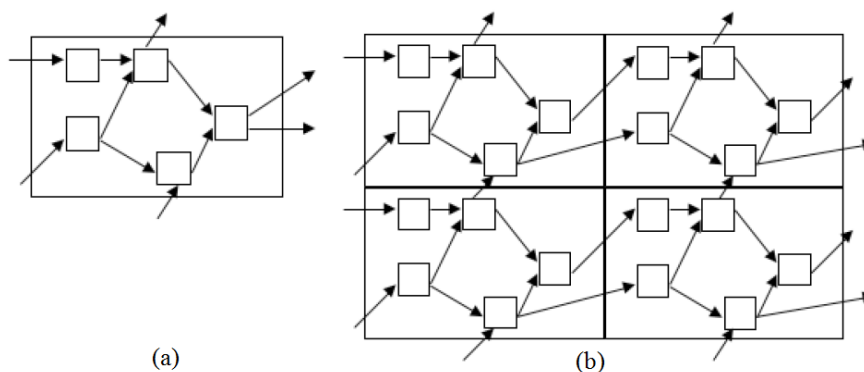
3

4

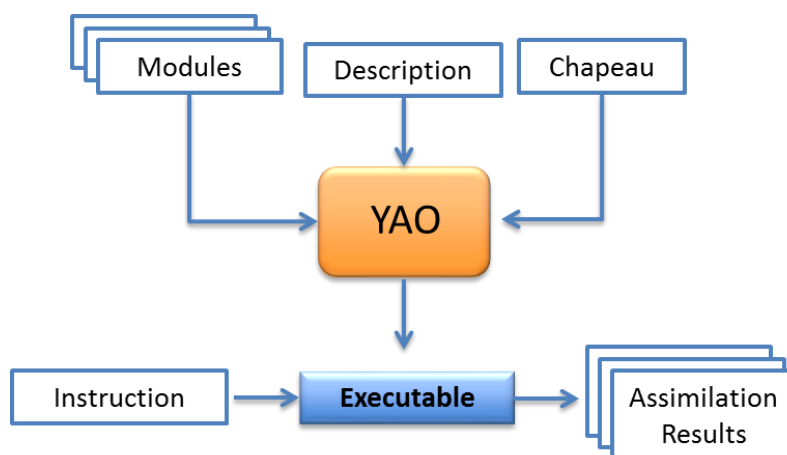
5 Table 5. Results for Experiment 3 (PFT 12). RMSE of model fluxes (a) and Parameters Relative errors (b) before and  
6 after the assimilation process, on FLUXNET Harvard Forest, 08 August 1996 during a week



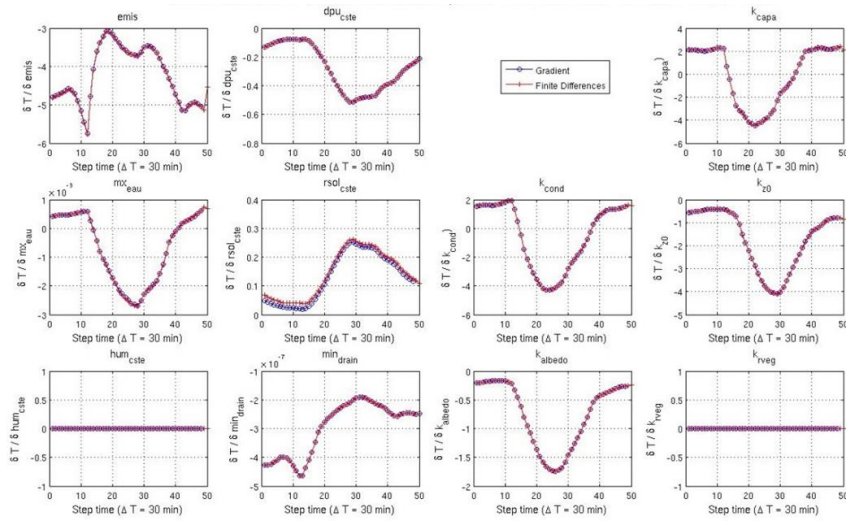
1  
2 Figure 1 (left) Example of a modular graph associated with four basic functions and five basic connections, three inputs  
3 points and three output points; (right) simplified description showing the acyclicity of the graph. Source: Nardi et al,  
4 2009



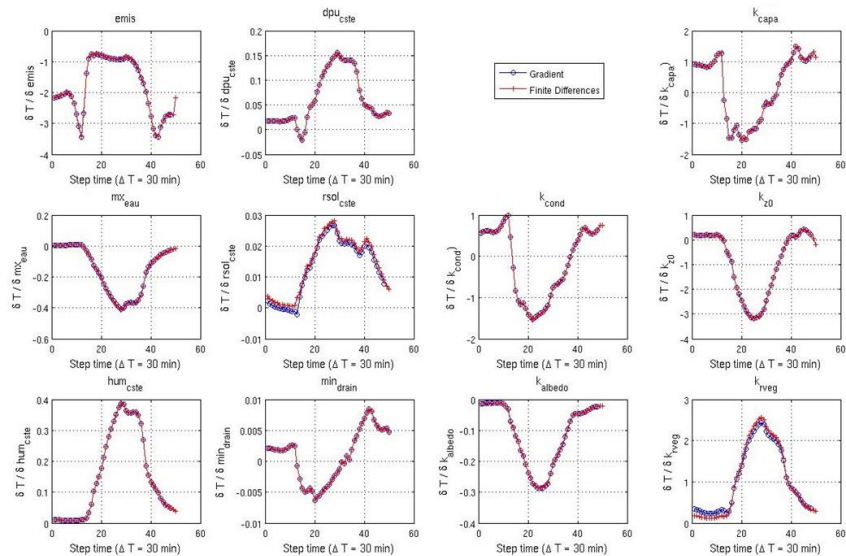
1  
2 Figure 2. (a) Example of a modular graph with five modules, assumed representative of the pointwise equations of a  
3 given model; (b) Partial view of the replication of the graph in space. Each elementary graph with five modules is  
4 associated with one grid point. Source: Nardi et al, 2009



1  
2 Figure 3. Structure of a project in YAO. The software generates an executable program from input modules, hat and  
3 description files. The generated program reads an instruction file to perform assimilation experiments.



(a)

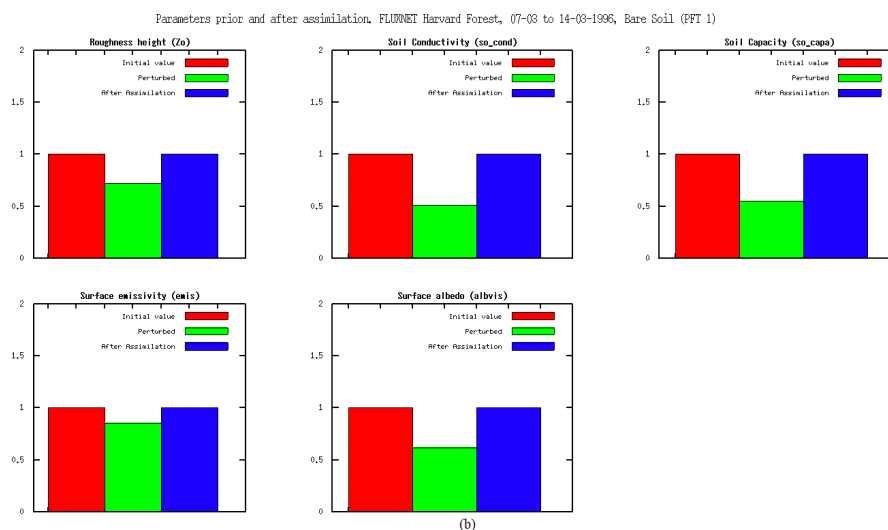
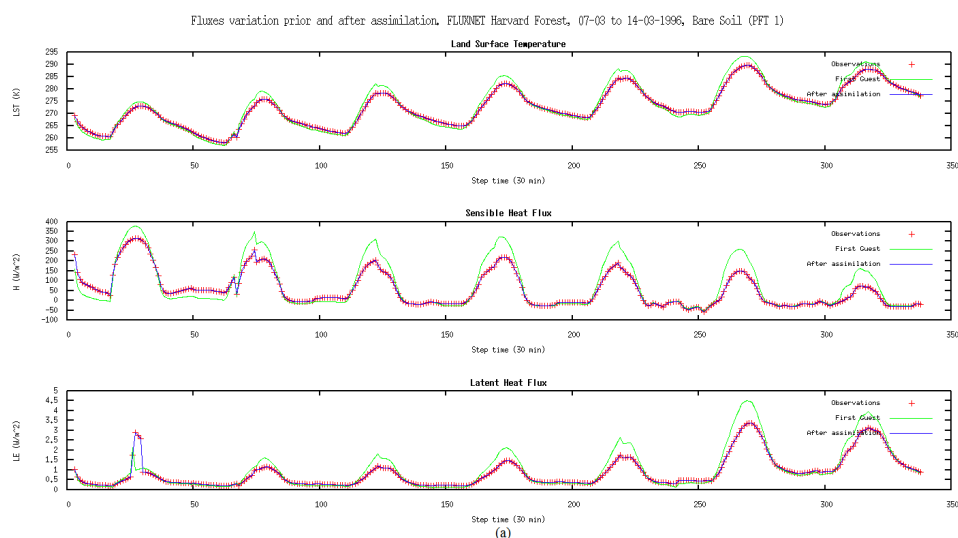


(b)

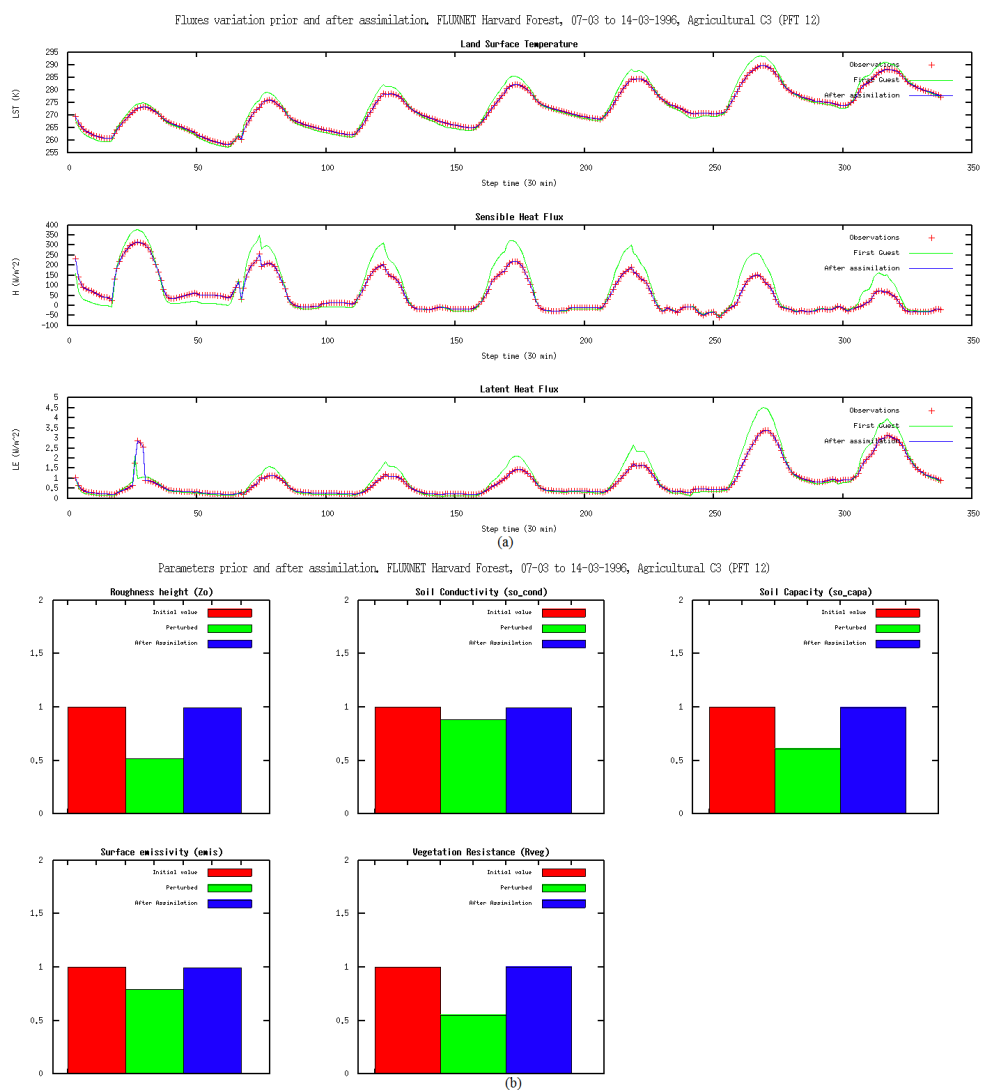
1  
 2 Figure 4. Comparisons for August 26,1996 at Harvard Forest, of the sensitivities obtained for each control parameter  
 3 with both the finite differences and the model gradients computed with the adjoint model. Sensitivity analysis results for  
 4 PFT 1 are in Fig.4 (a) and for PFT 12 in Fig.4(b). The sensitivities were computed on the surface temperature for  
 5 Harvard Forest. Blue curves represent the LST derivative with respect to each parameter given by the adjoint each half  
 6 hour over a day. Red curves represent the LST derivative computed with a finite difference discretization of the model.

7  
 8





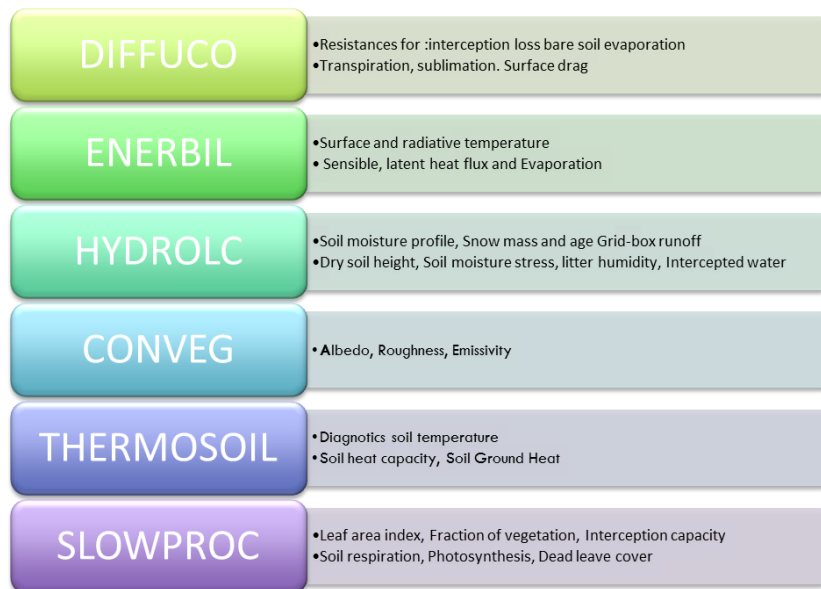
1  
 2 Figure 5. Comparison between variables and parameters prior and after assimilation, for experiment 1. LST, H  
 3 and LE are compared in Fig. 5.(a) and parameters values in Fig.5(b). Parameters values after assimilation  
 4 corresponds to values used to produce the synthetic observations and thus validating the twin experiment.  
 5  
 6



1  
 2 Figure 6. Comparison between variables and parameters prior and after assimilation, for experiment 2. LST, H  
 3 and LE are compared in Fig. 6.(a) and parameters values in Fig.6.(b). Parameters values after assimilation  
 4 corresponds to values used to produce the synthetic observations and thus validating the twin experiment.  
 5  
 6



1  
2 APPENDIX A  
3 **SECHIBA-YAO**  
4 The version of SECHIBA implemented in YAO includes the two-layer hydrology of Choisnel (1977), mentioned  
5 in Section 2. SECHIBA original code is implemented in a modular scheme, having a set of well-defined  
6 routines, independent in its processes and with a single entry point (a main routines handling the rest of the  
7 functionalities).  
8 A set of prognostic variables is defined for each module and its assignation depends on the forcing conditions,  
9 physics phenomena, etc. SECHIBA can work coupled with the other components of ORCHIDEE (STOMATE  
10 and LPJ) or it can be used offline, as it was used in this work. Once SECHIBA is coded in YAO, it can be easily  
11 coupled with the other modules of ORCHIDEE.  
12 In SECHIBA, the different routines were coded using Fortran language and can be run at any resolution and over  
13 any region of the globe. In the following, the version of SECHIBA implemented in YAO is denoted SECHIBA-  
14 YAO and the original version of the model, coded in Fortran, is denoted SECHIBA-Fortran. It can be run only  
15 one point at a time. ?  
16 ORCHIDEE uses MODIPSL and IOIPSL in its internal processes (see  
17 <http://forge.ipsl.jussieu.fr/igcmg/wiki/platform/documentation> for more information). Developed at IPSL, the  
18 first one is a set of scripts allowing the extraction of a given configuration from a computing machine and the  
19 compilation of the specific machine configuration components. MODIPSL is the tree that will host models and  
20 tools for configuration. IOIPSL helps to manage variables state history, variable normalization, file lecture, and  
21 among others.

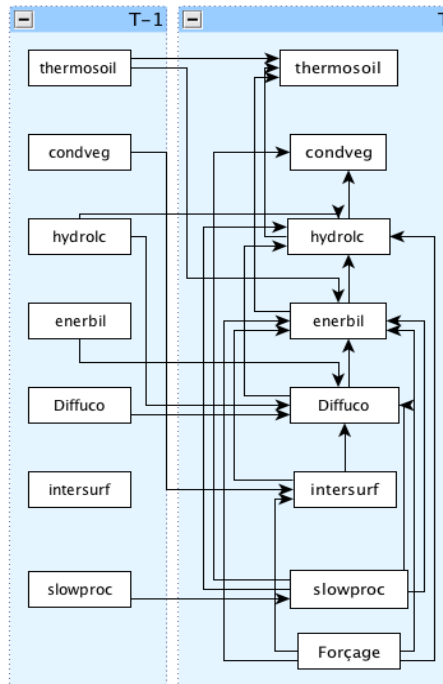


22  
23  
24

Figure A1 SECHIBA subroutines and its corresponding outputs. Source: Benavides, 2014.



1 The main routines in SECHIBA-Fortran are presented in Fig A1. These are also the routines considered in the  
2 YAO implementation of the model. First, DIFFUCO computes the diffusion and plant transpiration coefficients  
3 based on the atmospheric conditions, solar fluxes, dry soil height, soil moisture stress and fraction of vegetation.  
4 ENERBIL corresponds to the energy budget module. Surface energy fluxes related to the soil are computed,  
5 based on atmospheric conditions, radiative fluxes, resistances, surface type fractions and surface drag.  
6 HYDROLC is the hydrological budget module, taking as inputs the rainfall, snowfall, evaporation components,  
7 soil temperature profile and vegetation distribution. CONDVEG helps in the computation of the vegetation  
8 conditions. The thermodynamics of the model is computed in THERMOSOIL, based on a seven-layer soil  
9 profile. Finally, SLOWPROC computes the soil slow processes. When SECHIBA is decoupled from  
10 STOMATE, this module deals also with the LAI evolution.



11  
12 Figure A2 SECHIBA hyper graph, showing general model dynamics. Source: Benavides, 2014  
13

14 The different SECHIBA components are interconnected as shown in Fig.A2. The output of the different modules  
15 serves as inputs for the next one, thus resulting in an interdependency among modules to be considered when  
16 modeling SECHIBA-YAO.  
17